

Enhanced hydrogen solubility in niobium films

S. Moehlecke,* C. F. Majkrzak, and Myron Strongin
Brookhaven National Laboratory, Upton, New York 11973

(Received 9 August 1984)

The solubility of hydrogen in niobium films (100–3000 Å) and multilayers of Nb and Pd (20–130 Å) has been studied as a function of film thickness by resistivity and x-ray measurements. The H concentration in solid solution was observed to be greatly enhanced, by a factor of more than 40, as the Nb films were made thinner. This suggests a dependence of the phase diagram on film thickness, with a depression of the Nb-H critical temperature for films thinner than 1200 Å, but approaching the bulk values for thick films ($t > 2200$ Å). Similar results were observed in Nb-Pd multilayers.

In this paper, we report the observation of large hydrogen uptake in solid solution in thin films of Nb covered with Pd, and in multilayers of Nb and Pd.¹ It is suggested that the solid-solution region is greatly extended, probably by a lowering of the critical point, as already measured in thin films of Pd. In the work on Pd films, it is argued^{2,3} that in a film the boundary conditions greatly influence the interaction energy between hydrogen atoms,⁴ and thus the phase diagram. In a sample with free boundaries, the interaction between hydrogen and the metal is attractive, and for a perfectly clamped sample it can be repulsive. Although the Pd work demonstrates a lowering of the critical point in films, large increases in solubility were not reported. For Nb, an increase in room-temperature concentration in solid solution from 3% in bulk niobium to 130% in a film approximately 400 Å thick has been observed. In addition, these effects persist in multilayers of niobium and palladium, and hence there is actually a chance for a new kind of hydrogen storage material. This work describes both resistivity and x-ray diffraction studies of Nb films (100–3000 Å), covered with a constant-thickness Pd overlayer, and multilayers of Nb and Pd (alternating Nb and Pd layers both with the same thickness, from 20–130 Å).

The Nb films were grown by dc magnetron sputtering with Ar (2×10^{-3} Torr) at room temperature (the background pressure was 10^{-8} Torr). The sample substrates, regular microscope glass slides (3 in. \times 1 in.), and thin microscope glass covers (1 in. \times 1 in.), were mounted on a horizontal disk, which rotated back and forth over the Nb and Pd magnetron guns (both with deposition rates of 10 Å/s). All the Nb films (from 100–3000 Å) have a constant Pd overlayer thickness of 100 Å to protect the Nb from oxidation, and to provide a high hydrogen uptake rate.⁵

The impurity concentration in the Nb films was less than 1%, as shown by the resistance ratio of about 2–3. A superconducting transition temperature of 9.2 K was obtained for a thick film (3000 Å).

Two standard x-ray diffraction patterns ($\theta:2\theta$ scans) of the Nb-Pd multilayer films were obtained, one with the scattering vector \mathbf{K} parallel to the plane of the film (transmission geometry), and the other with \mathbf{K} perpendicular to it (reflection geometry). The x-ray data clearly show that both materials grow with a preferred orientation or crystallographic direction normal to the plane of the substrate. In the case of Nb this direction is [110], and for Pd it is [111] [these correspond to the close-packed planes for bcc and fcc (face-centered cubic) structures, respectively].

Rocking curves indicate a mosaic spread of the order of a few degrees. However, within the plane of the film, there is a random orientation of microcrystallites about the [110] Nb or [111] Pd axes, which are normal to the film plane. A grain size of approximately 50–100 Å was inferred from the measured widths of the x-ray diffraction peaks in the transmission geometry, and from transmission electron micrographs. For single bilayer films, a preferred orientation perpendicular to the substrate was observed, which was identical to that seen in the multilayer samples. However, transmission measurements were not done to establish whether or not any preferred orientation occurred in the film planes.

The H solubility measurements, which comprise the main part of the data, were made in the Nb films using two techniques: first, by monitoring the electrical resistance change due to H absorption *in situ* immediately after the film was made; and second, by following continuously the x-ray spectrum change with time due to H desorption in air after loading the films and multilayers with a high H concentration, which was out of thermodynamic equilibrium.

Figure 1 shows the measured percentage voltage change due to H absorption, which is proportional to the resistance since the current was constant, versus the Nb film thickness for a constant pressure (6×10^{-6} Torr) and temperature (300 K) in thermodynamic equilibrium. Since the voltage change is proportional to the resistance or resistivity change, we can relate the voltage change to the concentration through the relation that $C(\text{H}/\text{Nb}) = \Delta V / 4.33 V$.⁶ For a thin film this bulk relationship must be normalized to the resistivity of the film. If we assume that Matthiessen's rule is valid, one can write that $C(\text{H}/\text{Nb}) = \rho_F \Delta V / (4.33 \rho_B V)$, where ρ_F and ρ_B are the film and bulk resistivities. To get C from Fig. 1, one must have some idea of ρ_F / ρ_B . At 1100 Å, $\rho_F / \rho_B \approx 2.5$ whereas at ≈ 150 Å $\rho_F / \rho_B \approx 4.9$. Hence, at 1100 Å, $C \approx 16\%$, and at 150 Å, $C \approx 48\%$. From Fig. 1 we can see, in general, a large increase in the H concentration in solid solution as the Nb film thickness is decreased. Higher H pressures show similar curves, but with higher voltage changes for the thinner films. All the pressure-concentration isotherms (10^{-8} – 10^{-2} Torr) measured for each Nb film of Fig. 1 show an opposite deviation from Sievert's law (which states that $C \propto P^{1/2}$) than that observed for bulk Nb,⁷ i.e., it eventually becomes harder to put H in the film, and the pressure must be increased. However, we emphasize that even though P must be increased, the solid solution range increases. For a film 2150 Å thick, which

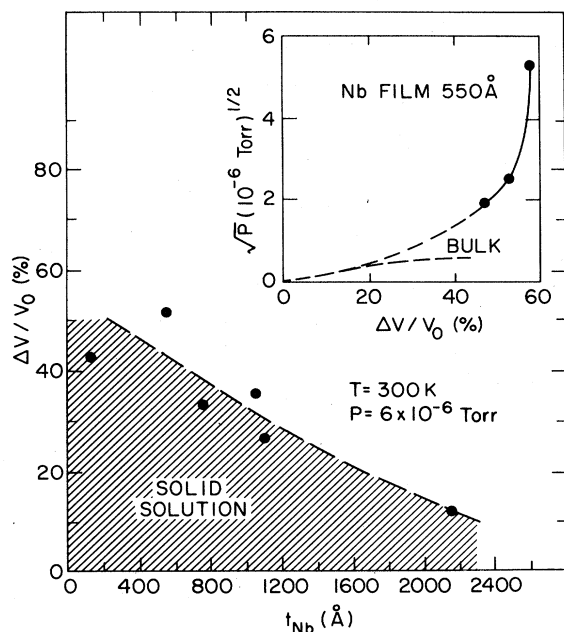


FIG. 1. Voltage change in percentage, due to H absorption, plotted as a function of Nb film thickness covered with Pd (100 Å) for a constant pressure (6×10^{-6} Torr) and temperature (300 K). The shaded area is the H solid-solution phase. The insert shows a pressure-concentration isotherm for a 550 Å Nb film. It can be seen that the deviations from Sievert's law (bulk curve) are significant, and are opposite to the usual deviations found in the bulk. Note that $\Delta V/V_0$ is related to $C(\text{H}/\text{Nb})$ by the relationship $C(\text{H}/\text{Nb}) = \rho_F \Delta V / (4.33 \rho_B V_0)$. Some characteristic values of ρ_F / ρ_B are given in the text.

showed hydride formation for H pressures higher than 10^{-6} Torr, the usual deviation from Sievert's law was observed, as expected for an attractive interaction. The shaded area under the curve of Fig. 1 is believed to be H in solid solution, because no change in the slope of the resistance with H absorption was observed. This would be expected to be due to a current redistribution if a second-phase (hydride) precipitation occurs.⁸

In Fig. 2, the x-ray results are summarized. The maximum lattice-parameter expansion is shown versus Nb film thickness, after loading all the films under the same conditions at approximately one atmosphere of H in air at room temperature. After exposing the film to air for several days, the Pd surface gets dirty, and is probably contaminated with CO and moisture. This makes the H desorption slower, taking several hours or days, and allows x-ray measurements to follow the slow desorption. It should be mentioned that the original H absorption and desorption rates could be recovered by resputtering a thin Pd layer on the top of the dirty Pd surface. Here, in Fig. 2, we observe a large increase in the amount of H absorbed as the film thickness is decreased. The H concentration, in at.%, shown on the right-hand side of Fig. 2, was calculated assuming the known bulk relation⁹ $C(\text{H}/\text{Nb}) = 17.24 \Delta a / a_0$ is valid for the films, where a_0 is the lattice parameter of the unhydrogenated Nb film. The shaded area under the curve of Fig. 2 indicates the region of H in solid solution. The data shown in Fig. 2 were obtained by monitoring the change in the po-

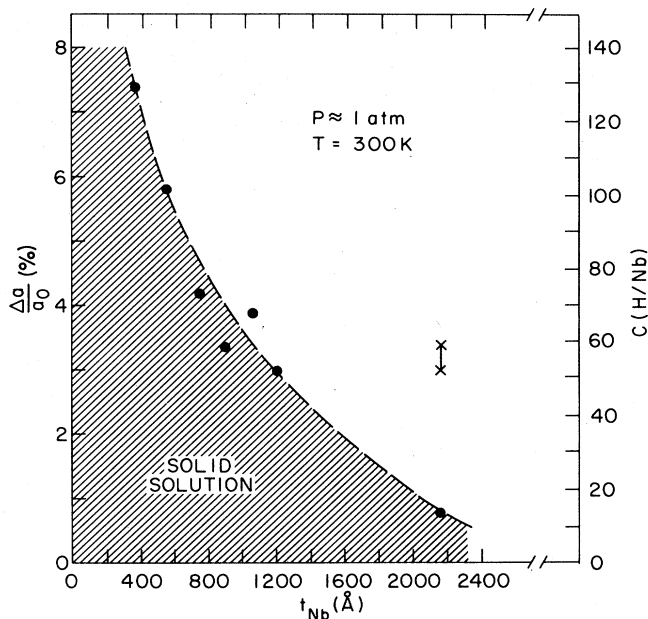


FIG. 2. Lattice-parameter expansion in percentage, due to H absorption vs Nb film thickness covered with Pd (100 Å) for a constant pressure (≈ 1 atm) and temperature (300 K). H concentration, in at.%, is calculated from the lattice-parameter change. The shaded area is the H solid-solution phase.

sition of x-ray diffraction peaks ($\theta:2\theta$ scan, reflection geometry) with time, as hydrogen diffused out of the samples initially loaded as described above. Except for Nb film thicknesses in excess of about 2000 Å, diffraction peaks corresponding to the orthorhombic β NbH_x phase were never seen. Instead, a continuous shift in position of a single diffraction peak of relatively constant intensity with time, to the original Nb(110) peak position occurred. This behavior is consistent with an identification of the diffraction peak as that of $\text{NbH}_x(110)$ in the α or α' phase above the critical temperature. For a film 2150 Å thick, however, a region of coexistence of two phases was observed as indicated by the presence of two distinct diffraction peaks (see Fig. 2), and a change of intensities following the lever rule. Owing to the crystallite size and/or strain broadening of the diffraction lines, it was not possible to identify this second phase, presumably β or α' . Films thicker than 2200 Å pulverize when hydrogenated, which indicates that they are approaching the bulk Nb-H behavior. For the thin films of Fig. 2, cycling with H showed an improvement in the total amount of H that a sample would take, due to a smaller final lattice parameter, $a_{[110]}$, after each cycle. No systematic variation of a_0 (unhydrogenated) with thickness was observed in these films, but in general an a_0 larger (by about 1.5%) than the bulk value was measured. During some x-ray measurements, we also monitored the resistivity change with time, and not only were the H concentrations calculated from the resistivities in reasonable agreement (to within $\approx 15\%$) with those calculated from the lattice parameters, but the results determined both ways had the same time-dependent behavior.

For the Nb-Pd multilayers, x-ray measurements were made only for H desorption (as described above for the sin-

gle bilayers) in the thick multilayers ($> 100 \text{ \AA}$ each layer) where both Nb[110] and Pd[111] peaks were well resolved, in order to avoid the interference effects which occur for the thinner multilayers. These results show the same general behavior observed before, i.e., a greatly enhanced solubility of hydrogen in the Nb layers, while the Pd layers show a large shift in the hydride phase boundary, e.g., from 61 at.% for bulk Pd to 38 at.% for a multilayer with 130 \AA layer thickness. It was also observed that all the hydrogen diffuses out of the Pd layers into the Nb layers before they desorb. An x-ray diffraction scan of a Nb-Pd multilayer sample in the transmission geometry (scattering vector \mathbf{K} in the plane of the film) was also obtained with the result that the expansion of the Nb[110] plane spacing along \mathbf{K} , due to the absorption of hydrogen, was the same as that measured in the reflection geometry (with \mathbf{K} perpendicular to the plane of the film). This implies that the unit cell is expanding uniformly in the two orthogonal directions. It was also observed that the Nb(200) plane spacing expanded by an amount consistent with maintaining a (110) plane spacing that is $\sqrt{2}$ times larger (as expected for a bcc structure).

A lowering of the Nb-H critical point temperature T_c , with thickness, was similarly observed in Pd-H films (Refs. 2 and 3), and is consistent with the weakening of the attractive H-H interaction noted from the pressure-concentration isotherms mentioned before. Theoretical studies^{10,11} of the hydrogen-metal phase-diagram dependence of sample dimensions¹² and boundary conditions are being analyzed to see if they can account for the large effects seen here. It is apparent that the explanation of all these results, particular-

ly the observation that films thinner than 1200 \AA (where presumably T_c is below room temperature) show an increase in H content in solid solution, is not completely understood. Plausible causes such as the boundary conditions imposed by the film-substrate interface and its extension throughout the multilayer, a lattice-parameter gradient along the film thickness, an anisotropic strained structure,¹³ and grain size effects are currently being investigated. It should be emphasized that if "clamping" of the film boundaries is indeed the explanation of these results, then it is interesting to note that this "clamping" occurs in the multilayers even with many tens of layers.

In summary, we have grown Nb films and Nb-Pd multilayers (superlattice), with preferred orientation, that show much larger H absorption in solid solution than bulk materials. For example, in a film 400 \AA thick it is found that the solid-solution phase contains at least 130 at.% H, compared with only about 3 at.% in bulk Nb. This is presumably due to a phase-diagram change, as the film is made thinner, with the critical point on the phase diagram going below room temperature.

We are grateful for discussions with many colleagues, and especially S. M. Shapiro and D. O. Welch. This work is supported by the Division of Materials Sciences, U.S. Department of Energy under Contract No. DE-AC02-76CH00016. The work of S.M. was supported in part by Conselho Nacional de Desenvolvimento Científico e Tecnológico (CNPq), Brazil and Fundação de Amparo a Pesquisa do Estado de São Paulo (FAPESP), Brazil.

*On leave from Universidade Estadual de Campinas (UNICAMP), 13100 Campinas, São Paulo, Brazil.

¹S. Moehlecke, C. F. Majkrzak, and M. Strongin, *Bull. Am. Phys. Soc.* **28**, 876 (1983).

²G. A. Frazier and R. Glosser, *J. Less-Common Met.* **74**, 89 (1980).

³R. Feenstra, G. J. de Bruin-Hordijk, H. L. M. Bakker, R. Griessen, and D. G. de Groot, *J. Phys. F* **13**, L13 (1983).

⁴G. Alefeld, *Ber. Bunsenges. Phys. Chem.* **76**, 746 (1972).

⁵M. Pick, J. W. Davenport, M. Strongin, and G. J. Dienes, *Phys. Rev. Lett.* **43**, 286 (1979).

⁶M. Strongin, J. Colbert, G. J. Dienes, and D. O. Welch, *Phys. Rev.*

B **26**, 2715 (1982).

⁷H. Zabel and J. Peisl, *J. Phys. F* **9**, 1461 (1979).

⁸J. A. Pryde and C. G. Titcomb, *Trans. Faraday Soc.* **65**, 2758 (1969).

⁹H. Pfeiffer and H. Peisl, *Phys. Lett.* **60A**, 363 (1977).

¹⁰H. Wagner and H. Horner, *Adv. Phys.* **23**, 587 (1974).

¹¹H. A. Goldberg, *J. Phys. C* **10**, 2059 (1977).

¹²H. Zabel and H. Peisl, *Phys. Rev. Lett.* **42**, 571 (1979).

¹³D. B. McWhan, M. Gurvitch, J. M. Rowell, and L. R. Walker, *J. Appl. Phys.* **54**, 3886 (1983).